

Supplementary Information for

Flexible and Transparent Gold Network Electrodes on Fluorinated Graphene

Yuna Lee[‡]^a, Eunji Ji[‡]^b, Minjung Kim^b and Gwan-Hyoung Lee^{*a}

^a Department of Materials Science and Engineering, Seoul National University, Seoul, Republic of Korea, E-mail: gwanlee@snu.ac.kr

^b Department of Materials Science and Engineering, Yonsei University, Seoul, Republic of Korea

Supplementary Figures:

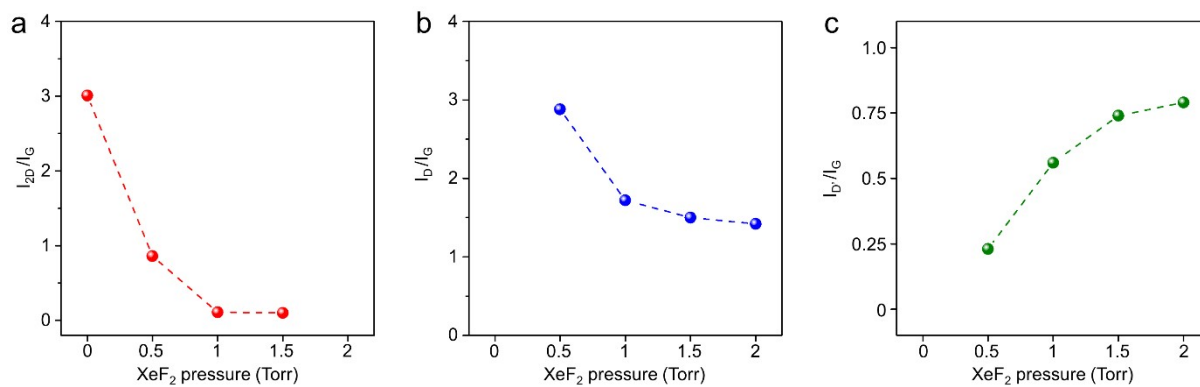


Figure S1. Raman Intensity ratio of fluorinated graphene (FG) under different XeF₂ condition (a) 2D/G peak (I_{2D}/I_{G}), (b) D/G peak ($I_{\text{D}}/I_{\text{G}}$) and (c) D'/G peak ($I_{\text{D}'}/I_{\text{G}}$)

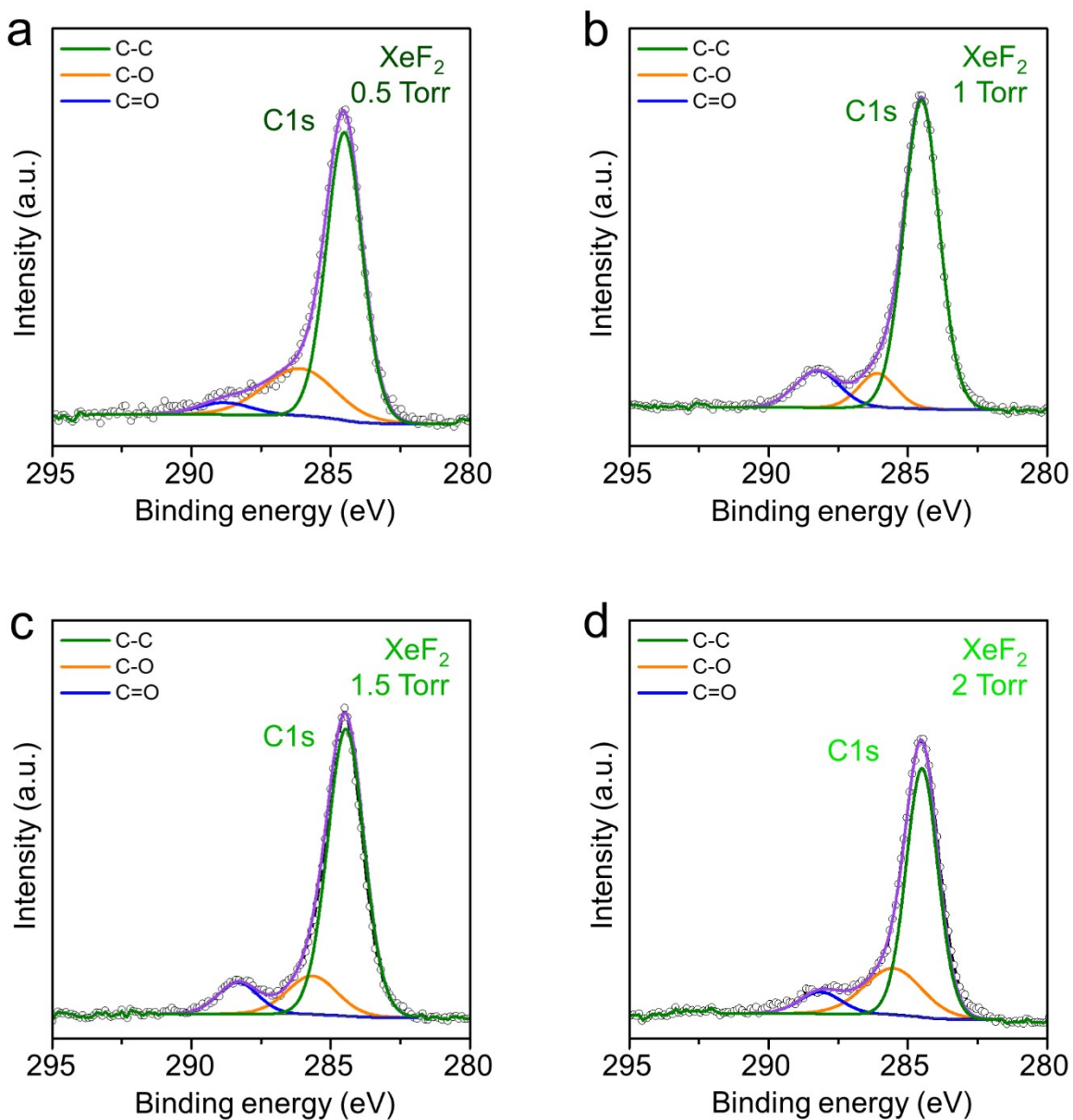


Figure S2. XPS spectra of C1s peak in CVD graphene after XeF₂ gas exposure (black circles) (a) 0.5 Torr (b) 1Torr, (c) 1.5 Torr and (d) 2 Torr.

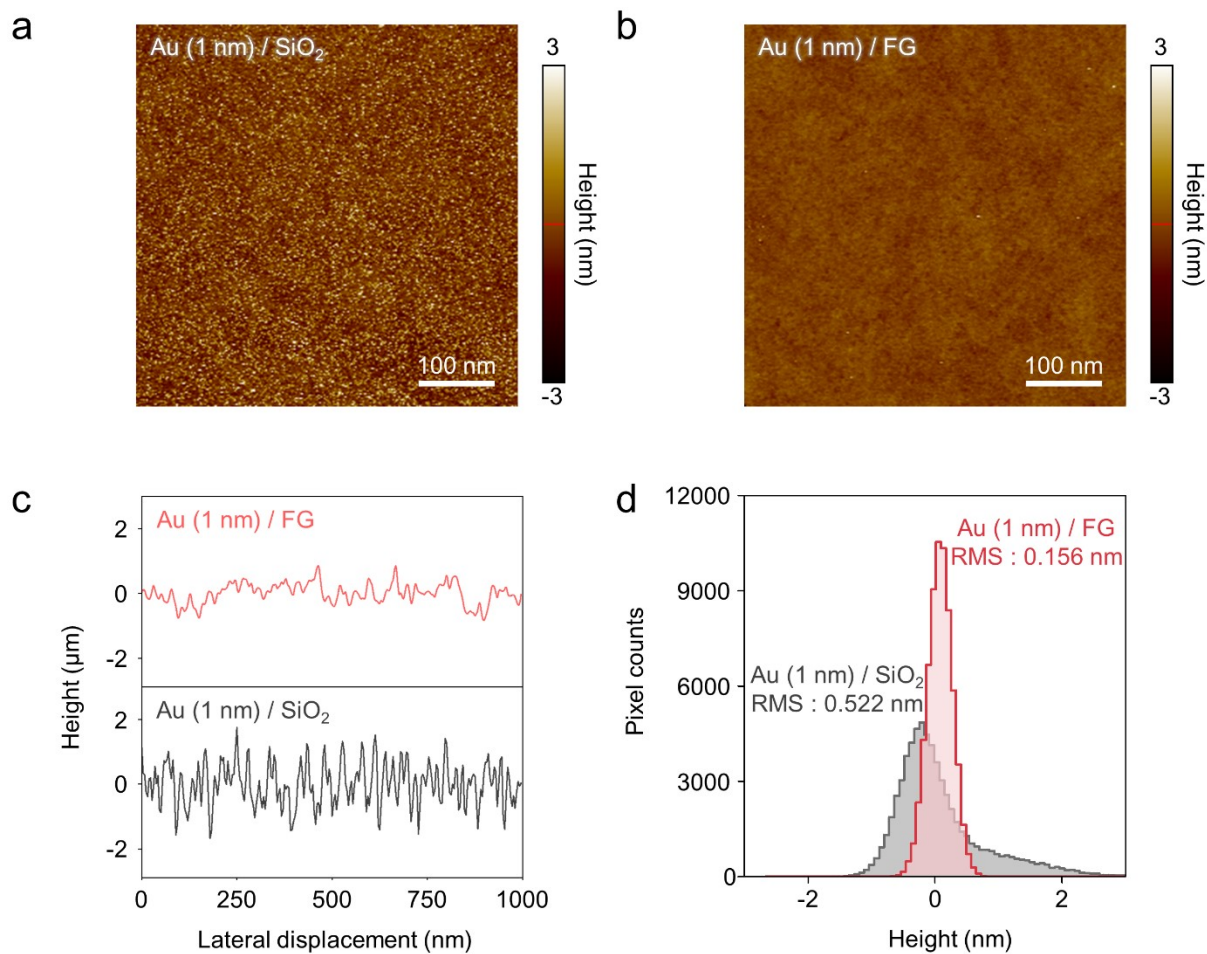


Figure S3. AFM image of Au (1 nm) on (a) SiO₂ and (b) FG. (c) Height profile of Au (1 nm) on SiO₂ and FG. (d) Histogram of the height distribution (surface roughness) of Au (1 nm) on SiO₂ and FG

Table S1. Raman Intensity ratio (2D/G peak (I_{2D}/I_G), D/G peak (I_D/I_G) and D'/G peak ($I_{D'}/I_G$)) of fluorinated graphene (FG) under different XeF₂ condition. The values highlighted in red are measured by different etcher (etcher 2), and the XeF₂ conditions are vary with changes in the equipment. However, the trend in Raman intensity ratios remains consistent.

	I_{2D}/I_G	I_D/I_G	$I_{D'}/I_G$
Pristine graphene	3.01	-	-
0.5 Torr_10s_5cyc	0.86	2.88	0.23
1.0 Torr_10s_5cyc	0.11	1.72	0.56
2.25 Torr_5s_60cyc (Etcher 2)	0.10	1.60	0.65
2.25 Torr_40s_60cyc (Etcher 2)	-	1.50	0.74
1.5 Torr_10s_5cyc	-	1.50	0.74
2 Torr_10s_5cyc	-	1.42	0.79
2 Torr_10s_10cyc	-	1.35	0.94

Mechanism of gold deposition depending on fluorination level

Surface defects can act as nucleation sites for deposited metals due to various physical and chemical properties. Defects typically provide sites with lower potential energy compared to the surrounding atoms, allowing metal atoms to minimize surface free energy upon reaching the defect sites. Additionally, the distortion of spatial and electron distribution of defects can enhance interactions with metal atoms, facilitating the diffusion of metal atoms to the defect sites and increasing the probability of metal deposition at these sites.¹⁻⁴

Therefore, fluorinated graphene through XeF₂ treatment can result in the formation of C-F sp³ bonds that can act as nucleation sites for metal. At low fluorination level (low sp³ defect density), the deposited gold atoms preferentially adhere to pre-existing gold clusters, promoting the growth of gold clusters. In contrast, at high fluorination level (high sp³ defect density), gold atoms preferentially deposit on nucleation sites associated with C-F sp³ bonding, forming new isolated small gold clusters. Subsequent deposition of more gold atoms leads to the formation of thick mesh structures with high porosity on weakly fluorinated graphene, while on highly fluorinated graphene, the resulting structures are thin meshes with small porosity.

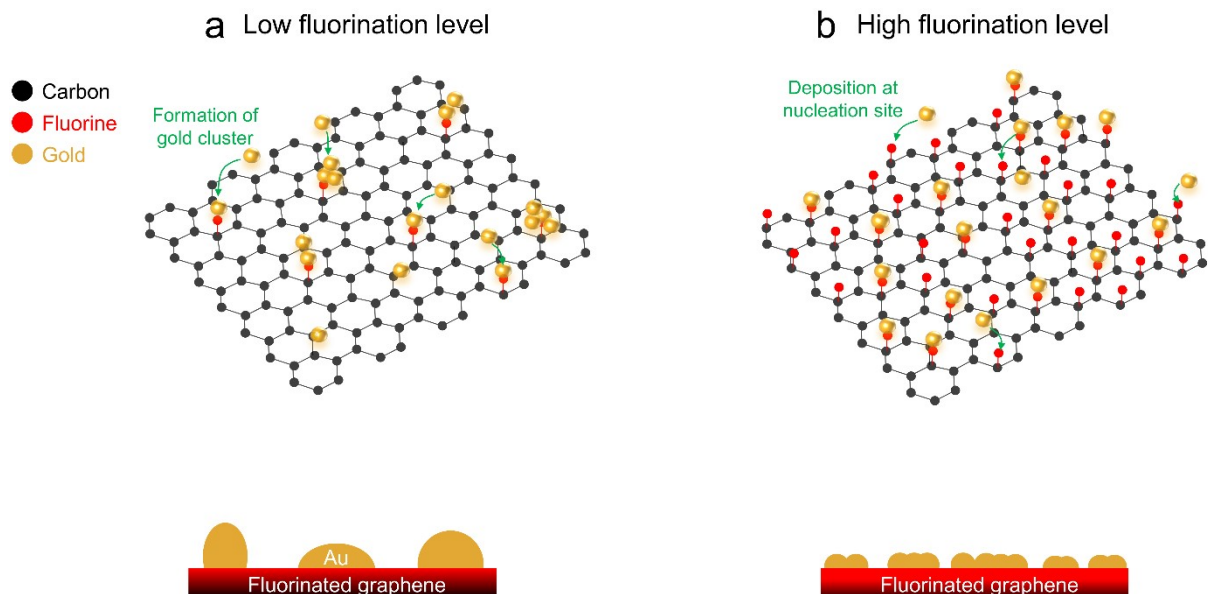


Figure S4. Schematic image of gold deposition depending on fluorination of graphene (low fluorination level (a) and high fluorination level (b))

Quantitative analysis of pores on gold network electrodes

For each I_D/I_G condition, we performed quantitative analysis of the pore distribution of Figure 4a. Porosity is calculated as the void area divided by the total area, with the highest porosity observed at the lowest coverage ($I_D/I_G = 1.5$). As the I_D/I_G ratio decreases, the metal coverage increases, resulting in decrease of porosity (Figure S5a).

Figure S5b represent the variation in the pore size distribution at Figure 4a depending on the I_D/I_G . At $I_D/I_G = 1.5$, which corresponds to the highest porosity, the number of small pores ($<250 \text{ nm}^2$) is the lowest, and there are 11 large pores ($>1000 \text{ nm}^2$) with $\sim 2276.29 \text{ nm}^2$ of largest pore. In the case of $I_D/I_G = 1.42$, there are 4 large pores ($>1000 \text{ nm}^2$) and the largest pore is approximately 1572.98 nm^2 . At $I_D/I_G = 1.35$ (lowest porosity), the number of small pores under 250 nm^2 is the highest, and the largest pore is $\sim 873.46 \text{ nm}^2$. The pore structure tends to exhibit smaller width as the I_D/I_G ratio decreases. This is due to the increase of C-F bonding on graphene surface, which causes the metal to fill the void and increase in coverage. Consequently, it indicates that as the degree of fluorination increase, the porosity and pore size decrease.

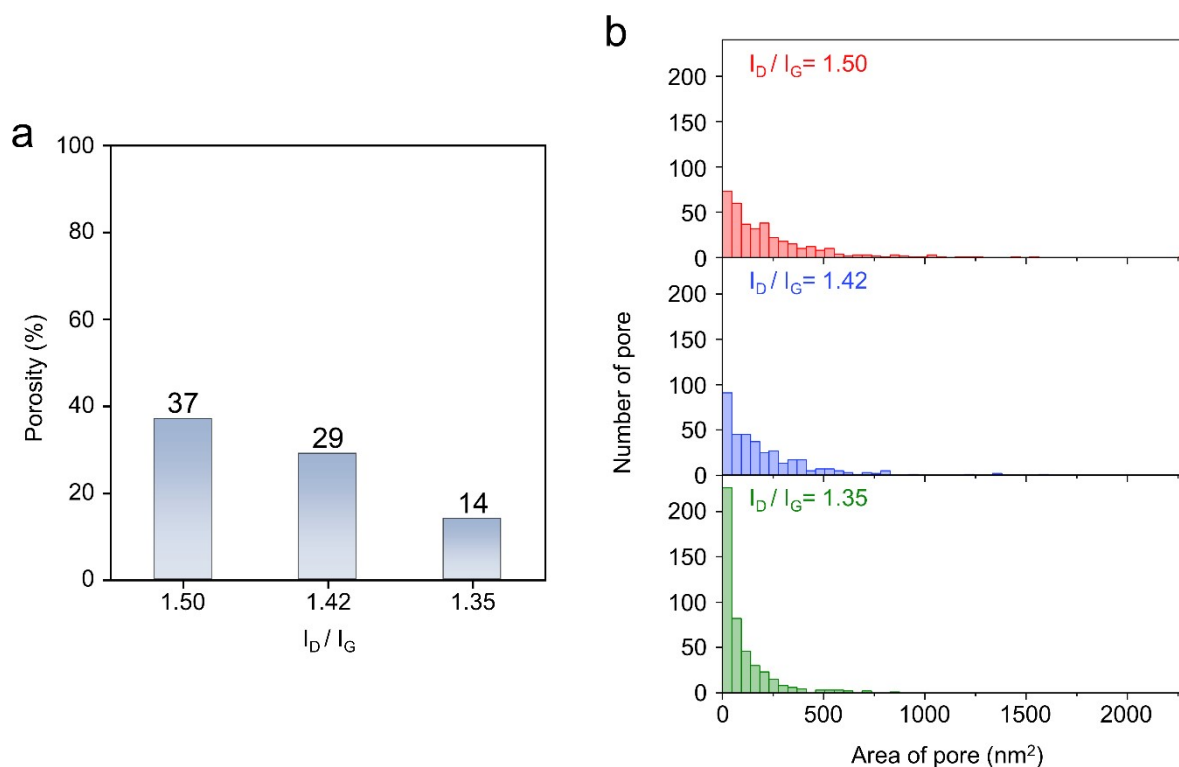


Figure S5. (a) Porosity (fraction of the area of void over the total area) of 5 nm Au/FG under each I_D/I_G condition. (b) Distribution of pore area of 5 nm Au/FG under each I_D/I_G condition.

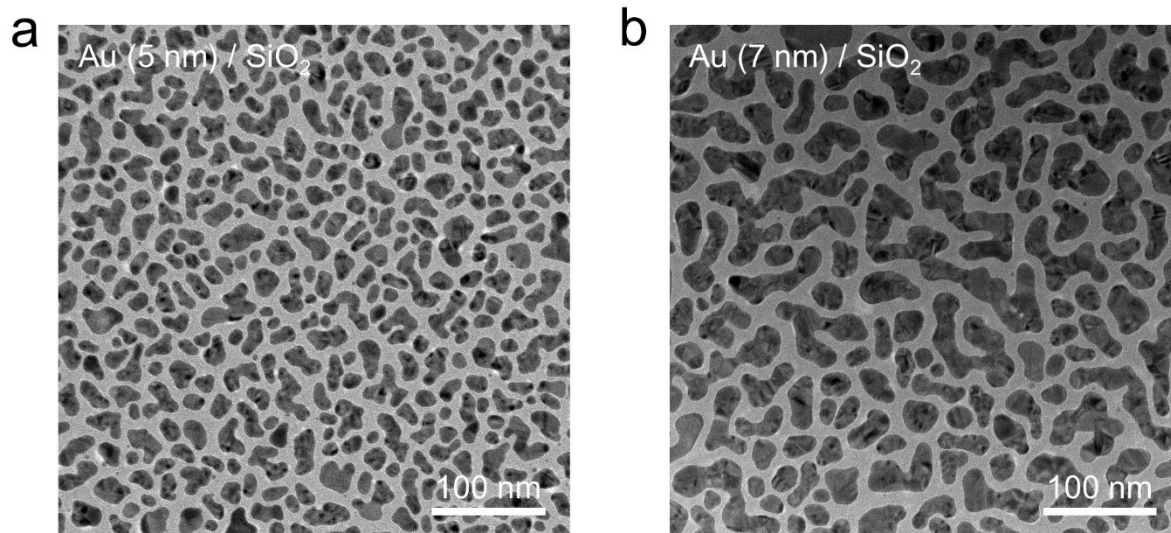


Figure S6. TEM image of (a) Au (5 nm) and (b) Au (7 nm) deposited on SiO₂.

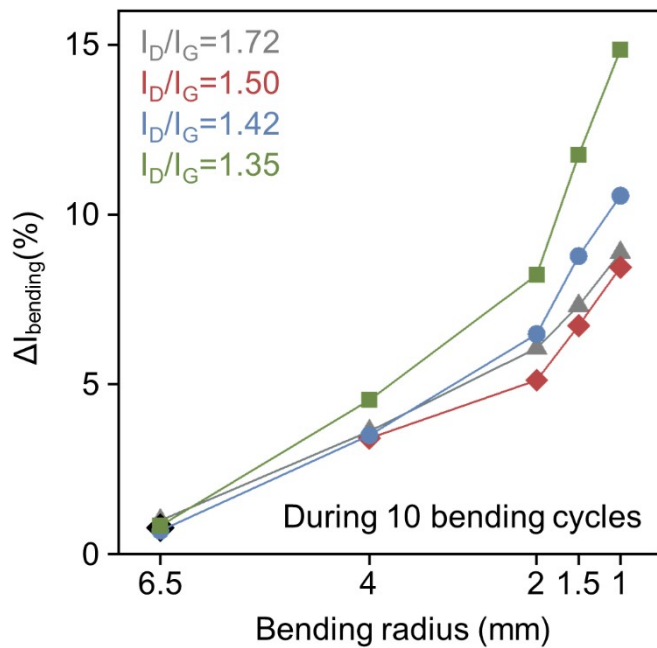


Figure S7. the percentage change in current of Au/FG electrode during bending ($\Delta I_{\text{bending}} = I_{\text{flat}} - I_{\text{bent}} / I_{\text{flat}}$). I_{flat} corresponds to the measured current when the electrode is in flat state while I_{bent} represents the measured current when the electrode is bent.

References

1. C. A. Campos-Roldán, G. Ramos-Sánchez, R. G. Gonzalez-Huerta, J. R. Vargas Garcia, P. B. Balbuena and N. Alonso-Vante, *ACS applied materials & interfaces*, 2016, **8**, 23260-23269.
2. J. Venables and J. Harding, *Journal of Crystal Growth*, 2000, **211**, 27-33.
3. W. Wallace, B. Min and D. Goodman, *Topics in Catalysis*, 2005, **34**, 17-30.
4. B. Min, W. Wallace, A. Santra and D. Goodman, *The Journal of Physical Chemistry B*, 2004, **108**, 16339-16343.